Isı Bilimi ve Tekniği Dergisi, 36, 2, 19-28, 2016
J. of Thermal Science and Technology

ISSN 1300-3615

PARAMETRIC INVESTIGATION OF A CENTRIFUGAL SLURRY PUMP WHILE HANDLING CLEAR WATER

Mehmet Salih CELLEK[*] and Tahsin ENGİN[**]
[*]Heat and Thermodynamics Division, Department of Mechanical Engineering, Mechanical Engineering Faculty, Yildiz Technical University, 34349 Besiktas, Istanbul, mscellek@yildiz.edu.tr
[**]Department of Mechanical Engineering, Applied Fluid Mechanics Laboratory, Faculty of Engineering, Sakarya University, 54187 Sakarya, engint@sakarya.edu.tr

(Geliş Tarihi: 04.04.2016, Kabul Tarihi: 03.05.2016)

Abstract: The performance of centrifugal slurry pump impellers strongly depends upon the complex configuration of the asymmetrical flow-field in the axial direction which is highly unsteady. The flow-field, in turn, is considerably affected by design parameters of volute casing and impeller geometry. Although many studies have focused on their optimization in water pumps, few studies have been conducted about centrifugal slurry pumps. The current study investigates the performance of a centrifugal slurry pump experimentally and numerically on, using clear water instead of slurry mixtures to avoid the effects of nonlinear intense the slurry mixtures. Additionally, a parametric study is carried out numerically to investigate the effects of blade configuration on the performance of slurry pump. Blade number, blade height and blade thickness are considered as the affecting parameters.

The results show that the increase in blade number leads to an increase at head and shaft power. However, the hydraulic efficiency is variable and depends on flow rates. Around operation conditions of the studied pump, the impellers which have three and four blades are more efficient than impellers with two and five blades. Furthermore, by increasing of blade height from 30 mm to 50 mm, the performance of the slurry pump increases only at high flow rates. On the other hand with the decreases in blade thickness from 50 mm to 30 mm, the performance of centrifugal slurry pump increases at all flow range.
Key words: Slurry pump, Parametric study, Blade number, Blade height, blade thickness

BİR SANTRİFÜJ ÇAMUR POMPASININ TEMİZ SU İLETMESİNİN PARAMETRİK İNCELENMESİ

Özet: Santrifüj çamur pompası çarklarının performansı eksenel yönde kararsız olan asimetrik akış alanının kuvvetle karmaşık konfigürasyonuna bağlıdır. Akış alanıda sırasıyla dizayn parametreleri olan salyangoz gövde ve çark geometrilerinden önemli ölçüde etkilenir. Bu geometrilerin optimizasyonu için su pompalarında birçok çalışma yapılmasına rağmen, çamur pompaları ile ilgili az sayıda çalışma yapılmıştır. Bu çalışma doğrusal olmayan yoğun çamur karışımlarının etkilerinden kaçınmak için çamur yerine temiz su kullanılarak, bir santrifüj çamur pompası performansını deneysel ve sayısal olarak incelemektedir. Bunun yanında kanat konfigürasyonun çamur pompası performansı üzerindeki etkileri incelenmesi için sayısal olarak bir parametrik çalışma gerçekleştirilmiştir. Pompa performansına etki eden parametreler olarak kanat sayısı, kanat yüksekliği ve kanat kalınlığı dikkate alınmıştır.

Sonuçlar kanat sayısının artması, basma yüksekliği ve mil gücünde artışa neden olduğu fakat hidrolik verimin ise değişkenlik gösterdiğini ve debiye bağlı olarak değiştiğini göstermektedir. Pompa çalışma şartlarında, 3 ve 4 kanatlı çarklar 2 ve 5 kanatlı çarklardan daha verimlidirler. Ayrıca kanat yüksekliğinin 30 mm'den 50 mm'ye arttırılması çamur pompasının performansını sadece yüksek debilerde artırmaktadır. Öte yandan kanat kalınlığının 50 mm'den 30 mm düşürülmesi çamur pompasının performansını tüm debi aralığında arttırmaktadır.
Anahtar Kelimeler: Çamur pompası, Parametrik çalışma, Kanat sayısı, Kanat yüksekliği, Kanat kalınlığı

NOMENCLATURE

D	diameter [m]
K	constant
L	length [m]
P_{sh}	shaft power [kW]
Q	flow rate [m^3/h]
T	torque [N.m]
V	Velocity [m/s]
b	blade height [m]
f	friction factor
g	gravity [m/s^2]
h	load [mwc]
k	turbulance kinetic energy [m^2/s^2]

n number of revolutions per minute [s^{-1}]
p pressure [N/m^2]
t blade thickness [m]
u velocity [m/s]
z blade number

Greek Symbols

ε turbulance dissipation rate [m^2/s^3]
η pump efficiency
μ viscousity [kg/m· s]
ρ density [kg/m^3]
σ Prandtl number
ω rotating speed [rad/s]

Subscripts

eff dynamic effective viscosity
t turbulance viscosity
k prandtl number for k
ε prandtl number for ε

INTRODUCTION

Slurry

The combination of any liquid and solid particles creates the slurry. The characteristic and the flow properties of the slurry depend on the transporting liquid and the type, size, shape and the quantity of the solid particles. According to the solid particles distribution inside the flow, slurries can be grouped as non-settling or settling types. Non-settling slurries includes fine particles that can form stable homogeneous mixtures and they usually have low wearing properties. On the other hand, settling slurries are consisted by coarser particles and specified to as being heterogeneous. The characteristic of this type slurry is that coarser particle has a tendency to have higher wearing properties and forms the majority of slurry applications. Therefore, particular attention must be given to flow and pump selection (Warman International Ltd, 2000).

Slurry pumps

Centrifugal slurry pumps have been employed widely for pipeline transportation systems, due to their ability to economically carry large size abrasive solids, fine and coarse-grain solids such as coal, dirt and gravel in the dredging. The superiority of the centrifugal pumps are based on the high and consistent flow rate, simple and effective controllability and the favorable ratio of flow rate to model, and the low manufacturing and maintenance costs. On the other hand, slurry pumps are exposed to some negative circumstances, which result in decreasing the performance characteristics over the working life such as wearing of the impeller blades and the volute case (Gandi and Sing, 2001; Singh et al, 2011; Engin and Gür, 2001; Engin, 2000). Due to these disadvantages, the manufacturer takes some precautions. For instance, blades are designed thicker, and the volute and the impeller are covered by rubber material. Besides, the pump is operated at low specific speed. For these precautions, the performance of the slurry pump becomes worse compared to the water pump and optimization is required to improve their efficiency.

The number of slurry pump impeller blades usually varies between two and six depending on the size and the type of the particles in the slurry. Pumping coarse and large particles may result in blockages. In these cases two or three blades can be used instead of 5 and 6 blades. On the other hand, the number of impeller blades can be restricted by blade thickness due to the impeller rubber material. Generally closed type impeller is used for the slurry pump because of higher efficiencies and less disposed to wear in front liner region. But open type impellers are occasionally preferred for specific operations and smaller pumps (Warman International Ltd, 2000). In some special cases, the impeller can be modified in order to avoid wear such as reduced diameter and eye impellers. A special attention must be given to designing a slurry pump impellers, which affect the fluid flow field and wear rates throughout the pump (Warman International Ltd, 2000).

Slurry pump volute casings

Slurry pump casings are also sensitive to wear as much as the impeller. Therefore, these pumps must run at nominal speeds as far as possible. Because high impeller peripheral speed damages the casing should be less than 27.5 m/s to avoid the thermal breakdown of the liner, adjacent to the outer edge of the impeller (Warman International Ltd, 2000). The casing shape is generally of a semi-volute or annual geometry, with a large clearance at the cutwater. With the increase of open clearance of cutwater (tongue), the efficiencies of the casings decrease, however, it offers the best compromise in terms of wear life (Warman International Ltd, 2000).

Slurry pump material selection

The material selection for the pump liners and impellers are made from two basic types of materials that are elastomers and wear/erosion resistant cast alloys. There are three commonly used elastomers which are Natural Rubber, Polyurethane and Synthetic Elastomers (for chemical applications). The selection of these materials also depends on each special application (Warman International Ltd, 2000).

Literature

Various techniques have been developed by researchers to bring out the complex flow pattern focusing on the design of high performance through centrifugal pumps and centrifugal slurry pumps. Vocadlo et al., 1974; Cave, 1976; Burgess and Reizes, 1976; Sellgren, 1979; Gahlot et al., 1992; Engin and Gür, 2003; Kazim et al. (1997) have investigated the performance of the pump with different solid concentrations , different solid materials, particles size, specific gravity. Correlations to predict the head reduction factors for the centrifugal slurry pumps have been employed in these studies.

On the other hand, Kadambi et al., 2004; Charoennegam, 2001; Mehta, 2004; Mahiwan (2000) studied to visualize the flow in the centrifugal slurry pumps by means of particle image velocimetry technique (PIV) to investigate the flow pattern and the effects of slurry in the pumps.

Computational Fluid Dynamics (CFD) is progressively applied in the turbo machines such as compressors, turbines, fans and pumps. Recently, the complex and the high turbulence internal flows in pumps can be visualized employing of the CFD methods Thus, it is possible to minimize the undesired flow such as the secondary flow, flow separation, and vortex flow which will lead to energy dissipation. Recently, with the aid of CFD, some researchers have been investigating the performance of centrifugal pumps. Zhou et al. (2003) studied the effects of three blades profile on the centrifugal pump impeller. They suggested that the predicted results identified with the twisted-blade pump are better than the results identified with the straight-blade pump. It is also recommended to focus on improving the straight-blades design in the future. From the study of Shujia et al. (2006) on virtual performance of a centrifugal pump, the results indicated that the computational values obtained by Fluent using MRF and $k-\varepsilon$ turbulent model give better predictions in comparison with the experienced ones for a centrifugal pumps, particularly at the normal flow rate situation. Bacharoudis et al. (2008) studied the outlet blade angle with the same diameter range from 20 deg to 50 deg for a hydraulic laboratory pump. The pumps characteristic curves indicate that as the blade angle decreases from 50 deg to 20 deg the hydraulic efficiency of the laboratory pump increases. Furthermore, 20 deg has the best performance at the nominal flow rate. Jafarzadeh et al. (2011) investigated the turbulent models $k-\varepsilon$, RNG $k-\varepsilon$, RSM for a centrifugal pumps using CFD. Comparing both CFD and experimental data, the author recommended the RNG $k-\varepsilon$ turbulent model. In the study of Anagnostopoulos (2009) a commercial centrifugal pump was simulated with the turbulent flow in a two-dimensional using CFD software. A numerical optimization algorithm based on unconstrained gradient approach developed and combined with the evaluation software to find the impeller geometry which maximizes the pump efficiency using as free design variables the blade angles at the leading edge and the trailing edge. A fast and fully automated cartesian grid was proposed in order to accelerate the numerical design process for turbomachinery such as pumps and turbines. Chakraborty and Pandey (2011) studied the effects of different blade number on the performance of centrifugal pumps at high rotating speed. The result exhibits that with the increase of blade number, the total pressure and the head of centrifugal pump increased. However, the efficiency of the hydraulic pump with the blade number is changeable and complicated. Liu et al. (2009) investigated the effects of both particle concentration and particle diameter on flow in the FGD System Pump by using Fluent. They concluded that particle diameter has more influence than volume concentration in the distribution of particles and head will decline as a result of the increasing of volume concentration on the design point. Singh et al. (2011) had evaluated the performance characteristics of the centrifugal slurry pump with bottom ash with different concentration. They observed that the head and the efficiency of centrifugal slurry pump decreases with increase in solid concentration and numerically obtained results are reasonably satisfactory. Das et al. (2011) studied two dimensional flow phenomenon of a centrifugal slurry pump while it handles clear water for entire flow rate from shut-off to maximum flow rate comparing with the experimental data. They recommended that the selecting number of blades and blade thickness are very crucial for centrifugal slurry pumps and need to be examined.

Many investigations on the performance of centrifugal pumps are mainly limited to water pumps. A few ones actually related to slurry pumps briefly presented above. Effects of slurry concentration, the volume fraction of slurries; slurry particle diameters and slurry variation on the pump performance curves are mainly investigated. In additional to these characteristics, it is important to optimize the impeller configuration of the slurry pump. It is noticeable that the optimization of an available centrifugal slurry pump is rather limited in the literature.

In the present study, a centrifugal slurry pump is studied experimentally and numerically following a numerical parametric study in order to investigate the pump performance taking into account number of blades (2, 3, 4, 5), blade height and blade thickness for shroud type impeller. The flow field inside the pump is illustrated with pressure distribution contours and velocity streamlines. Additionally, the pump performance curves are compared and discussed. The Computational Fluid Dynamics analysis is carried out with the commercial software ANSYS Fluent (2012).

MODEL DESCRIPTION

Slurry pump geometry and parametric impellers

Centrifugal slurry pump and its CAD model simulated based on the data provided by Tufekcioglu Kaucuk Ltd. (2013) presented in Fig. 1 and Fig. 2. Due to the presence of solid particles and high density of the mixture at operation conditions, both volute casing and impeller are coated with a rubber material to avoid wear. This situation results in employing thicker blade and less number of blades in the centrifugal slurry pump. The rubber coated shroud type impeller, which has 3 backward blades, is presented in Fig. 1 (b) without upper disk. The outlet blade angle is approximately 30°. The blade height is constant ($b_1 = b_2 = 30$ mm) and the mean blade thickness is 50 mm. The pump geometry consists of three main parts namely inlet part, impeller part and volute casing part. The inlet part is the simplest one in which fluid enters. The volute casing is just as critical as the impeller for converting velocity to pressure. The outward velocity of the water slows as it is pushed against the volute, resulting in an energy transfer

from the kinetic energy of water to its potential energy Cengel and Cimbala (2006). The discharge of the volute is circular and the fluid flow is throughout in radial direction. The blade height and the blade thickness of the available impeller are shown in Figs. 1 (b) and (c). To investigate the effect of number of blades, blade height and blade thickness on the performance of the centrifugal slurry pump, nine impellers are parametrically created as shown in Fig.3.

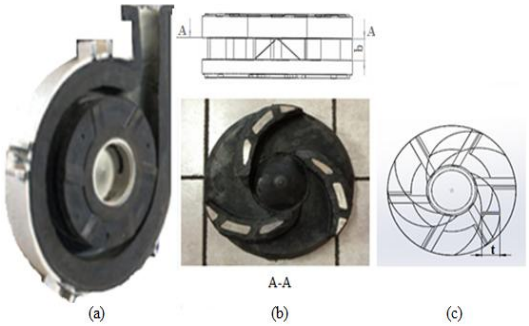

Fig 1. Original natural rubber coated centrifugal slurry pump (a) and impeller with blade height (b) and mean thickness of the blade (c) (Tufekcioglu Kaucuk Ltd, 2012)

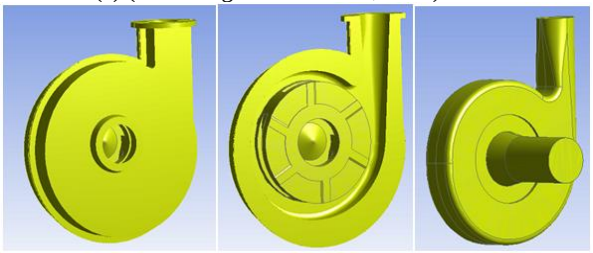

Fig 2. The slurry pump CAD geometry and fluid domain of the simulated centrifugal slurry pump

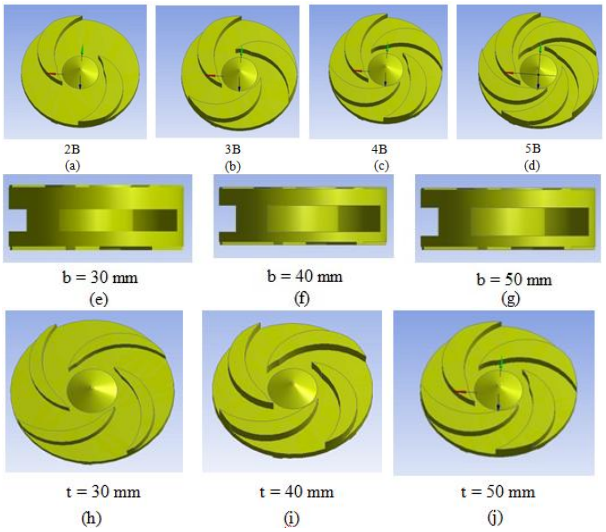

Fig 3. The parametrically created shroud type impellers with different blade numbers, blade height and blade thickness (The cross section of impellers (a),(b),(c),(d),(h),(i) and (j))

Mesh generation

ANSYS meshing (ANSYS ICEM CFD) was used to generate the mesh. Because of the complex geometrical model, the tetrahedral mesh was considered for three parts of the pump. Inflation layer meshing was applied to boundary layer region to capture the flow separation, pressure drop and adverse pressure gradients inside pump with sufficient ten layers. Proximity and curvature were used for the advanced size function and relevance center was adapted to medium for meshing tools. The minimum mesh number utilized for the suction inlet part is 51768. The rotary impeller part is the most critical one where mechanical energy transfers to fluid occur there. Due to the complex flow field through the impeller passage, 1591149 elements are used for this part. It should be noted that mesh element numbers of the impellers may have different values. The stationary volute, which converts the kinetic energy to potential energy, has also remarkable impact on the pump performance. It consists of 1088106 tetrahedral elements. There are 986558 total nodes and 2731023 total elements of 3B pump, shown in figure 4. A detailed mesh independence test was performed in the previous study by the authors (Cellek and Engin, 2016).

Computational method

The calculations are carried out with commercial finite volume software, Fluent which helps in achieving a solution for the steady and three dimensional incompressible Reynolds-averaged Navier-Stokes equations. The numerical algorithm is SIMPLE, in which the pressure parameter is discretized utilizing the second-order upwind scheme (Bacharoudis et al. 2008; Engin 2006).

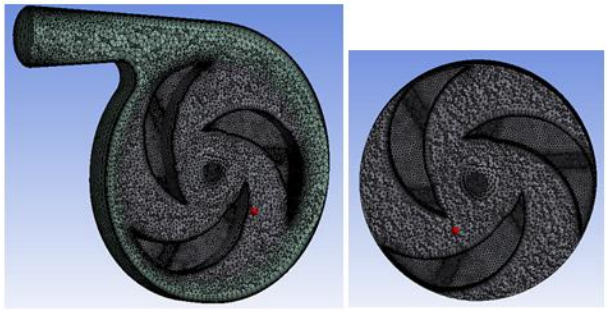

Figure 4. Mesh generation of the centrifugal slurry pump and 3B impeller clipped with a plane

Mathematical model

The three-dimensional incompressible flow through the impeller solved in a moving frame of reference with constant rotational speed. The flow through the stationary parts of the pump is solved in an inertial reference frame. The governing equations for the impeller are formulated as follows

$$\nabla \rho \mathbf{u}_r = 0 \quad (1)$$

$$\nabla \rho \mathbf{u}_r = 2\rho\boldsymbol{\omega} \times \mathbf{u}_r + \rho\boldsymbol{\omega} \times \boldsymbol{\omega} \times \mathbf{r} = -\nabla p + \mu_{eff}\nabla^2 \mathbf{u}_r. \quad (2)$$

$$\nabla \rho \mathbf{u} = -\nabla p + \mu_{eff}\nabla^2 \mathbf{u} \quad (3)$$

where $\mathbf{u}_r$ is the velocity vector, $\boldsymbol{\omega}$ is the rotational speed, p is the pressure, μ_{eff} is the dynamic effective viscosity which is a linear combination of laminar and turbulent viscosity derived from $k-\varepsilon$ model of turbulence. The differential transport equations for the turbulence kinetic

energy (k) and turbulence dissipation rate (ε) in the standard $k-\varepsilon$ model formulated below the values of k and ε can be directly obtained from these equations. In this equations $\mathbf{u}$ is the local velocity vector, G_k represents the generation of the turbulent kinetic energy due to the mean velocity gradients, σ_k and σ_ε are the turbulent Prandtl numbers for k and ε. Model constants used in the equations are $C_\mu = 0.09$, $C_{1\varepsilon} = 1.44$, $C_{2\varepsilon} = 1.92$, $\sigma_k = 1.0$, $\sigma_\varepsilon = 1.3$ (Shujia et al. 2006; Bacharoudis et al. 2008; Engin 2006).

$$\nabla\rho\mathbf{u}k = \nabla\cdot\left[\left(\mu+\frac{\mu_t}{\sigma_k}\right)\cdot\nabla k\right] + G_k - \rho\varepsilon \quad (4)$$

$$\nabla\rho\mathbf{u}\varepsilon = \nabla\cdot\left[\left(\mu+\frac{\mu_t}{\sigma_k}\right)\cdot\nabla\varepsilon\right] + C_{1\varepsilon}\frac{\varepsilon}{k}Gk - C_{2\varepsilon}\rho\frac{\varepsilon^2}{k} \quad (5)$$

$$\mu_t = \rho C_\mu \frac{k^2}{\varepsilon} \quad (6)$$

$$\mu_{eff} = \mu + \mu_t \quad (7)$$

Boundary conditions and assumptions

Turbulent flow is modeled employing standard $k-\varepsilon$ model, which has been widely utilized for turbulence model ranging from industrial to environmental flows (Zhou, 2003; Shujia, 2006; Bacharoudis et al. 2008; Anagnostopoulos, 2009; Chakraborty and Pandey, 2011; Liu et al., 2009; Singh et al., 2011; Das et al., 2011). In order to model the near wall treatment, the standard wall function is selected. Water is used as working fluid instead of multiphase flow in order to optimize pump parameters. Rotating impeller is taken as a rotating zone, with rotational speeds 900 rpm. The other zones are selected as stationary part. No-slip boundary conditions have been imposed over the impeller blades and the walls. Velocity inlet and pressure outlet boundary conditions are selected for the inlet and outlet, respectively. The turbulence intensity and the hydraulic diameter involved parameters are estimated with values of 5% and D, respectively.

Results and discussion

In this part, performance curves of the centrifugal slurry pump obtained experimentally are compared to CFD predictions under identical conditions. Then the results are obtained by the parametric study presented comparatively. The flow-field is considerably influenced by the impeller design configuration. Therefore, the fluid flow field revealed as 3-D.

Experimental work

In order to test the available slurry pump, an experimental set-up with three available units, was established at the company to test the different sizes of the pumps shown in Fig. 5. A water accumulator tank used to remove the air flow additionally ensures continuity for obtaining more accurate results within the system. Some devices are available on the test rig for the measurements. Two pressure transducers were employed to measure the suction and discharge pressures. Flow rate is measured with the use of an electromagnetic flow meter. Two shut-off valves are fitted on each test unit. Electrical signals corresponding to the measurement of flow rate, pressure and torque are read by data acquisition unit.

Figure 5. The experimental set-up (left) and the slurry pump (right), (Tufekcioglu Kaucuk Ltd., 2012)

In this study, the experimental and numerical test results are compared in Fig. 6. (a), (b) and (c). The pump head, shaft power and overall efficiency are calculated as function of flow rate. From the Fig. 6(a), it's observed that as the flow rate increases the total head of the numerical results decrease in compatible with experimental ones at on design condition (60 to125 m^3/h). Whereas the deviation of the head curves are increased at off design conditions which are at the low flow rates (25-60 m^3/h) and high flow rates (140-150 m^3/h). On the other hand, a little difference occurred between numerical and experimental shaft powers which directly affect the hydraulic efficiency. The best efficient point (bep) that the hydraulic efficiency of the slurry pump achieves its maximum value is selected approximately 125 m^3/h. It is observed from the characteristics curves that the minimum hydraulic efficiency deviation takes place at bep point, $125 m^3/h$. The CFD post processing results of the tested slurry pump are presented as 3B impeller whose blade height and blade thickness are 30 mm, 50 mm respectively.

The effects of blade number on the pump characteristics

The performance characteristics of the slurry pump with different blade number where water is the working fluid are presented in Fig. 7. (a),(b) and (c). It can be found that with the increase in blade number, the head of the slurry pump increases up to 100 m^3/h except for 5B impeller. After the 100 m^3/h flow rate, the situation becomes complicated. It means that the head of the 4B and 5B impellers decreases sharply while the head of the 2B and 3B decrease gradually. The pump head curves of the 2B and 3B impellers are steadier than the 4B and 5B impellers. From the polynomial head curves, it is noted that the decreases in the heads increases with the high flow rates. This situation is results from high frictional losses inside the impeller formulated with the aid of Bernoulli Equation as follows (Cengel and Cimbala, 2006).

$$\frac{P_1}{\rho g}+\frac{V_1^2}{2g}+z_1=\frac{P_2}{\rho g}+\frac{V_2^2}{2g}+z_2+\sum h_{losses} \quad (8)$$

$$\sum h_{losses}=\sum h_{friction}+\sum h_{local} \quad (9)$$

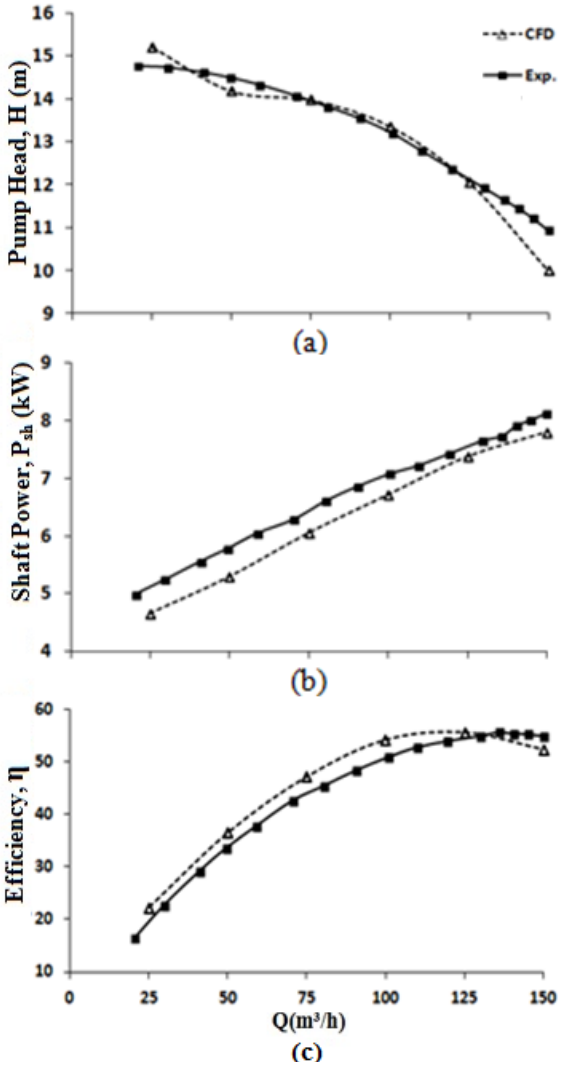

Figure 6. Measured and computed characteristic curves: (a) pump head-flow rate, (b) Pump shaft power-flow rate, and (c) pump overall efficiency-flow rate

$$h_{friction}=f\frac{L}{D}\frac{V^2}{2g}=f\frac{L}{D^5}\frac{16\cdot Q^2}{2g\pi^2}=K\cdot Q^2 \quad (10)$$

$$h_{local}=\sum K\frac{V^2}{2g} \quad (11)$$

$$h_{friction}=f(V^2) \text{ and } h_{local}=f(V^2) \quad (12)$$

Besides the head curves of the studied impellers, the comparison of the shaft power curves of the impellers is demonstrated in Fig. 7(b). It can be seen that the increment of flow rate result in increasing the pumps shaft power for each impeller. The increment in the blade number results in an increase in shaft power. Power consumption of 4B and 5B pumps are almost the same up to 75 m^3/h whereas it is the maximum for the 4B impeller at off design condition.

The efficiency of the 2B, 3B, 4B and 5B impellers as a function of flow rate are presented in Fig. 7(c). As for efficiencies, the efficiency of the 5B impeller is almost the worst at all whereas the efficiency of the 3B impeller is the best for all design conditions. The efficiency of the 4B

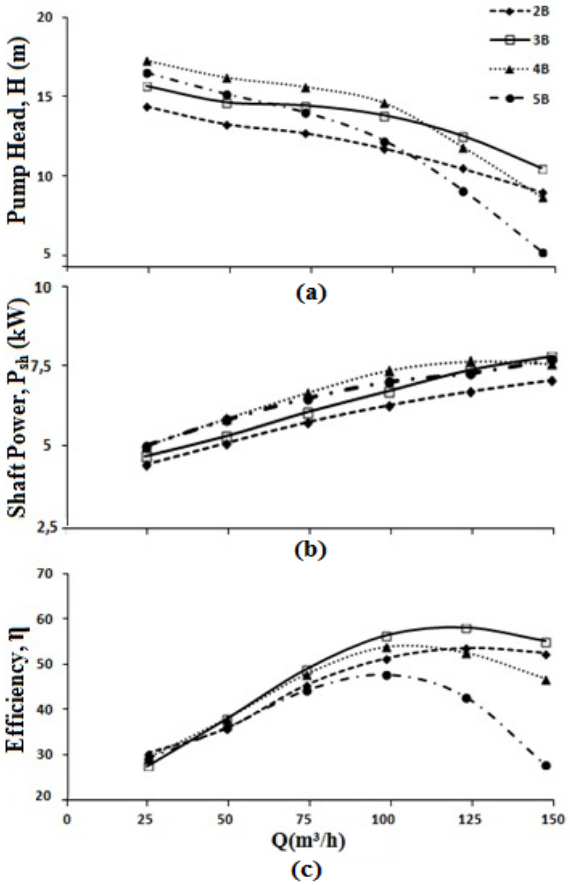

Figure 7. Characteristics performance curves of 2B, 3B, 4B and 5B impellers

impeller better than the 2B impeller up to 115 m^3/h but it is the opposite after this flow rate. The maximum efficiencies of the pumps are between 100 m^3/h and 125 m^3/h flow rates. It also can be observed that the efficiencies of 2B and 3B pumps are better than 4B and 5B pumps beyond the bep point. The reason is that the frictional losses increase with the increment in flow rates. Moreover frictional losses increase with increment in blade numbers owing to high velocities at the narrow flow passages.

The effects of blade height on the pump characteristics

Fig. 8 (e), (f), and (g) shows calculated heads, shaft powers and efficiencies as function of flow rate for 3B impellers with different blade height 30 mm, 40 mm and 50 mm. The predicted curves indicate that the head of impeller of h =50mm would be much better than those of impellers with h=40mm and h=30 mm. Moreover, the decrease in the head of h=30 mm impeller, more sharply than the others after the 100 m^3/h. This may indicate that the head of the pump is increased with the increment in the blade height. The shaft power increases almost linearly depending on the flow rates. It is clear that with

the increment in blade height increases the pump shaft powers.

As for efficiencies, it can be seen clearly that the efficiency of the h=30 mm impeller better than h=40 mm and 50 mm impellers up to 110 m^3/h whereas it is the worst at high flow rates (110-150 m^3/h). The efficiency of the 50 mm impeller is the maximum at high flow rates especially at 150 m^3/h. It is noticed that the increment in blade height shifts the bep points of the impellers towards the right side of the apsis.

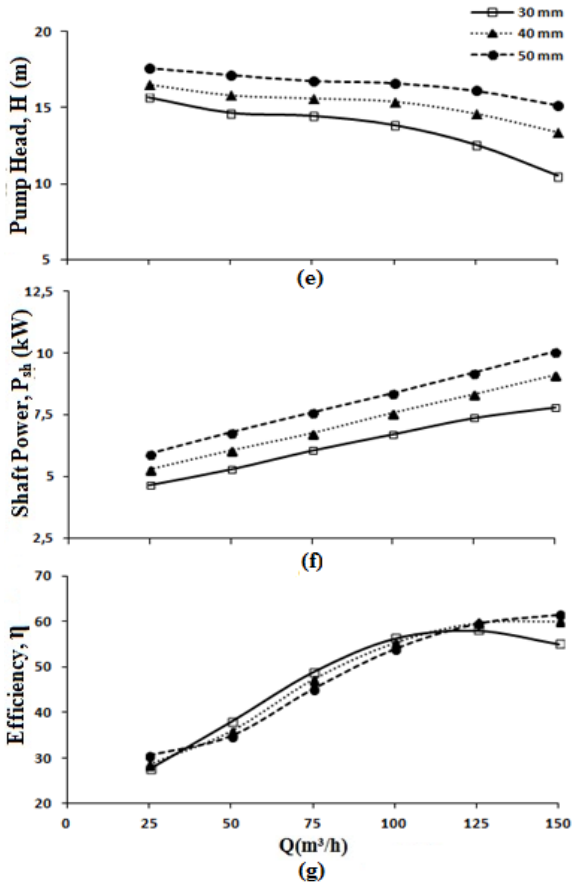

Figure 8. Characteristics performance curves of 3B impellers for 30 mm, 40mm, 50mm blade height

The effects of thickness of the blade on the pump characteristics

Another parametric study is related to the blade thickness which is directly influence pump performance. With the same boundary conditions and assumptions, the effects blade thickness can be investigated on the pump performance. Under the incompressible flow condition, the flow rate is constant, if impeller flow passage narrows, the velocity of the flow increases as a result of continuity theory. The hydrodynamic losses, consists of both frictional loss and local loss, increases with the increase of velocity as shown in Eqs. 9-12.

The predicted performance curves such as head-flow rate, shaft power-flow rate and efficiency-flow rate are presented in the Figs. 9 (h), (i) and (j). As it can be observed from these figures, the pump head is close to each other at low flow rates up to 75 m^3/h , however after this point with the increment of blade thickness a rather sharp inverse decrease is observed. As for the shaft power, with the increase of blade thickness the shaft powers are the same and do not change up to a certain flow rate, 75 m^3/h. After this point, especially after the 100 m^3/h, the shaft power of the 50 mm blade thickness decreases polynomial trendline where others decrease linearly. It is noted that although the frictional losses inside the 30 mm impeller is minimum, the required shaft power is almost maximum at the full range of flow rates. In spite of required more shaft power, the efficiency of the impeller, whose blade thickness is 30 mm, is the maximum almost at full range of flow range as expected. On the other hand the efficiency of the impeller (t=50 mm) is minimum almost all flow rates.

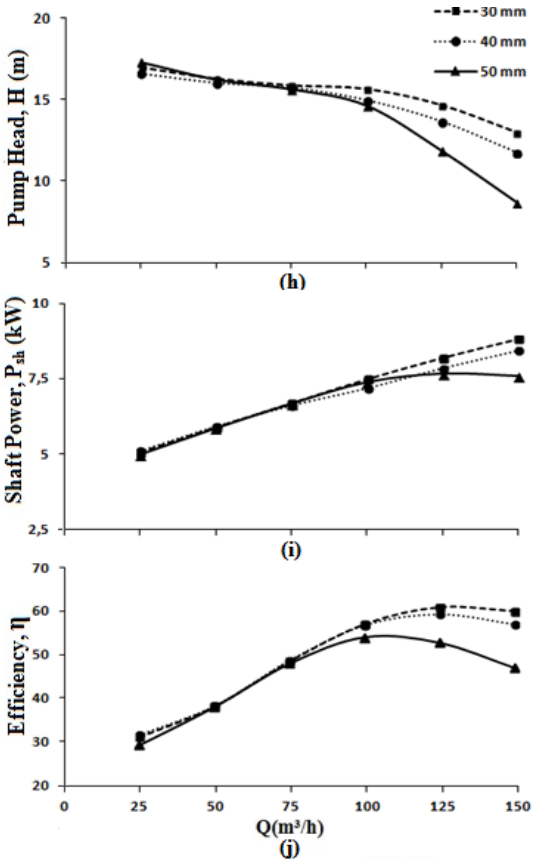

Figure 9. Characteristics performance curves of 4B impellers for 30 mm, 40mm, 50mm blade thickness

The post processing of CFD analysis of the studied pump

To see the interaction of the volute casing and the impeller, the flow field inside the pump can be illustrated with pressure distribution contours and velocity streamlines. The static pressure distribution contours for the considered slurry pumps are shown in Figs. 10, 11 and 12. It can be observed that the minimum static pressure takes place at the impeller suction side especially at the suction side of the blades for the each impeller and it is gradually increased towards to outer diameter of the impeller whereas the maximum static

pressure takes place at the outlet of the pump as expected. It is seen from the pressure contours that the pressure distribution on the volute casing is similar to each other. However, the situation is not the same for the impellers. With the increase of the blade number from 2 to 5, the static pressure inside the impeller suction becomes to decrease. The low pressure field inside the available impeller (3B) is gradually disappeared with the increasing of blade height. On the other hand with the increment in blade thickness, the low pressure field inside the available impeller is increasing.

Based on the impellers pressure contours, the pressurized and suction sides of the blades are obviously recognized. The low pressure field takes place at the suction side of the blades. If the pressure declines below the saturated vapor pressure at this region, the fluid vaporizes and forms small bubbles of gas which causes cavitation. The potential cavitation region for the some studied impellers is illustrated in Fig. 13. From the figures, the cavitation region is growing with the increase of number of blades at the same fluid temperatures, $T_{fluid} = 30^{\circ}$.

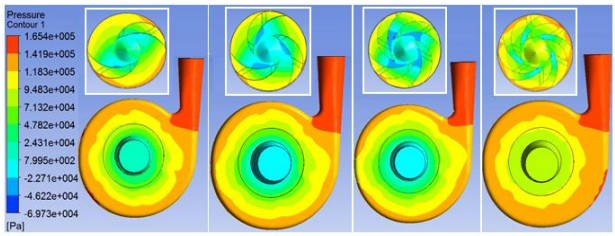

Figure 10. Pressure contours of the simulated pump with 2B, 3B, 4B and 5B impellers

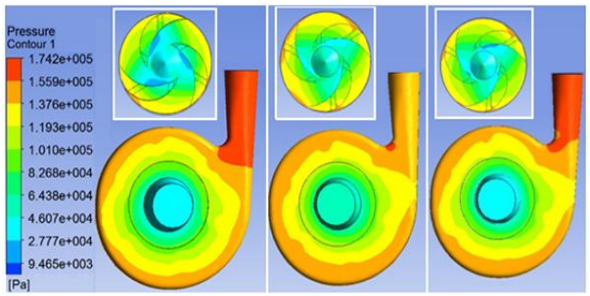

Figure 11. Pressure contours of the simulated pump with 3B impeller for 30 mm, 40 mm and 50 mm blade height

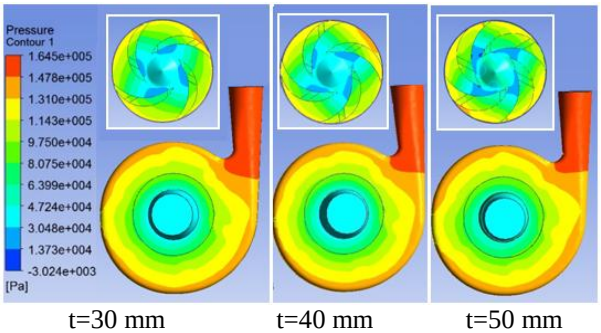

Figure 12. Pressure contours of simulated pumps for 4B impeller with 30 mm, 40 mm and 50 mm blade thickness

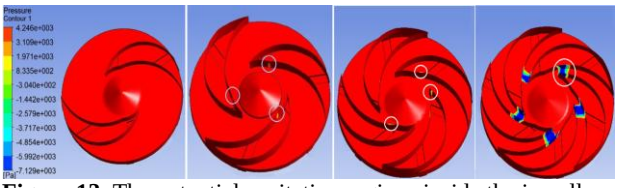

Figure 13. The potential cavitation regions inside the impellers for 2B, 3B, 4B and 5B impellers ($T_{fluid} = 30^{\circ}$)

The streamlines are quite useful due to pointing out the instantaneous aspect of fluid motion along the flow field. Furthermore, with the help of streamlines the flow separations or circulations in the fluid region can easily be detected. In this study, streamlines are also used to indicate the velocity distributions. Figs. 14 and 15 show the velocity streamlines inside the slurry pumps at the design point. From the streamlines it is observed that the flow is steadier while using 3B and 4B impellers then using 2B and 5B impellers. The minimum velocity is takes place at suction side of the impeller; the maximum velocity is located at the trailing edge of the blades inside the flow passage. The kinetic energy of the fluid is converted to pressure at the out of the volute as pump working principle. Therefore the velocity of the fluid is decreasing towards to outlet of volute. Flow separation can be observed at the pressure side of the leading edge of the blades the each impeller. The situation results from blade configuration especially leading edge of the blades and high velocities. Any flow phenomena such as secondary flow, vortex flow inside the pump is not obviously appearing. This situation may be stated due to low angular velocity and less number of blades. It should be noted that high pressures and velocities will gradually cause wearing while the flow becomes two phase due to the presence of the solid particles.

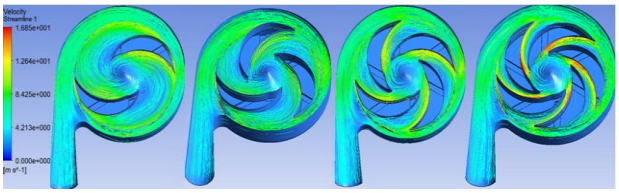

Figure 14. Velocity streamlines for the 2,3,4 and 5 impellers whose blade thickness are 50 mm

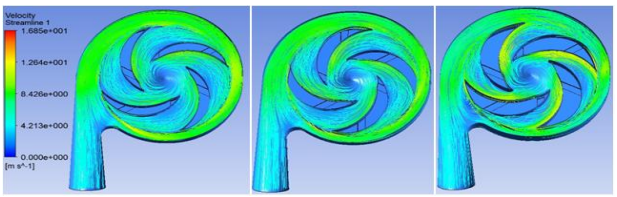

Figure 15. Velocity streamlines for 4B impellers whose blade thickness are 30 mm, 40 mm and 50 mm

CONCLUSION

This study has focused experimentally and numerically on the performance of a centrifugal slurry pump using clear water instead of slurry mixtures to avoid intensive nonlinear properties of slurry mixtures. A parametric study has been carried out numerically in order to investigate the effects of number of blades (2, 3, 4, 5), blade height (30mm, 40mm, 50mm) and blade thickness

(30mm, 40mm, 50mm) on pump performance for shroud type impeller. The flow field inside the pump is illustrated employing pressure distribution contours and velocity streamlines. Additionally, the pump performance curves are compared and discussed. The computational fluid dynamics analysis is performed with the commercial software Fluent, using the standard $k-\varepsilon$ turbulence model.

According to the results the blade number of a shroud type impeller of centrifugal slurry pump is a significant parameter affecting the pump performance. Considering the hydraulic efficiency at wide range of flow rate, 5B impeller exhibits the worst performance compared to the 2B, 3B and 4B impellers. On the other hand 3B impeller is the best one. Despite having highest head at wide range of flow rate (25-110 m^3/h), 4B impeller is not as efficient as 3B impeller. The hydraulic efficiency of 2B impeller is between 4B and 5B impellers up to 115 m^3/h flow rate but it is better than them at high flow rates (115-150 m^3/h).

The findings also showed that with the increase of available impeller blade height from 30 mm to 50 mm, both pump head and shaft power increase at full range of flow rates, however the hydraulic efficiency of centrifugal slurry pump increases only at high flow rates. On the other hand, decreasing in available impeller blade thickness from 50 mm to 30 mm leads to an increase in the head, the shaft power and the hydraulic efficiency of the pump remarkably at high flow rates, (75-150 m^3/h).

As a result, if the head of the available impeller (3B) is adequate, the selecting of 3B is the right among 2B, 3B, 4B and 5B impellers. But if it is not adequate, 4B impeller can be selected at low flow rates. On the other hand, if the pump operates at high flow rates, the blade height can be increased from 30 mm to 50 mm for the same impeller height because of obtaining high pump head and better hydraulic efficient. Moreover, if the blade thickness of the available impeller can decrease from 50 mm to 30 mm, the performance of the pump becomes the best.

ACKNOWLEDGEMENTS

The authors are thankful to Scientific and Research Council of Turkey (TUBITAK-TEYDEP-3110368) and Company of Tufekcioglu Kaucuk Ltd for their supports on this research.

REFERENCES

Anagnostopoulos J.S., 2009, A Fast Numerical Method for Flow Analysis and Blade Design in Centrifugal Pump Impellers, *Computers&Fluids 38,* 284-289.

ANSYS® Academic Research, Release 12.

Bacharoudis E.C., Filios A.E., Mentzos M.D. and Margaris D.P.,2008, Parametric study of a centrifugal pump impeller by varying the outlet blade angle, *The Open Mechanical Engineering Journal,* 2:1, 75-83.

Burgess K.E. and Reizes A., 1976, The effect of sizing, specific Gravity and Concentration on the performance of Centrifugal Pumps *Proc. Inst. Mech. Eng,* 190-36/76., 391-399

Cave I., 1976, Effects of Suspended Solids on the Performance of Centrifugal Pumps, *Proc. Hydro Transport-4, paper H3, BHRA Fluid Engineering.*

Cellek M.S. and Engin T., 2016, 3-D Numerical Investigation and Optimization of Centrifugal Slurry Pump Using Computational Fluid Dynamics, *Journal of Thermal Science and Technology, 36:1, 69-83.*

Cengel Y.A. and Cimbala J. M., 2006, *Fluid Mechanics Fundamentals and Applications*, McGraw Hill, New York.

Chakraborty S. and Pandey K. M., 2011, Numerical Studies on Effects of Blade Number Variations on Performance of Centrifugal Pumps at 4000 Rpm, *IACSIT International Journal of Engineering and Technology.*, 3:4, 410-416.

Charoennegam P., Kadambi J.R., Subramanian, A., Addie G., 2001, Investigation of slurry flow in a centrifugal pump using PIV, 4th International Conference on Multiphase Flow (ICMF-2001), New Orleans, La.

Das L.G., Rawat M.K. and Kuri N., 2011, Flow Analysis of a Centrifugal Slurry Pump While Handling Clear Water at Design and Off-Design Conditions, *The 11 th Asian International Conference on Fluid Machinery and The 3rd Fluid Power Technology Exhibition,* IIT Madras, Chennai, India, 21-23.

Engin T. and Gur M., 2001, Performance Characteristics Of a Centrifugal Pump Impeller With Running Tip Clearance Pumping Solid-Liquid Mixtures, *Journal of Fluids Engineering*, 123, 532-539.

Engin T., 2000, Eperimental Investigation of Centrifugal Pumps When Handling Solid-Liquid Mixtures, Institute of Science of Sakarya University.

Engin T., 2006, Study of Tip Clearance Effects in Centrifugal Fans with Unshrouded Impellers Using Computational Fluid Dynamics, *Proc. IMechE Vol. 220 Part A: Journal of Power and Energy*, 599-610.

Engin T., Gur M., 2003, Comparative Evaluation of Some Existing Correlations to Predict Head Degradation of Centrifugal Slurry Pumps, Journal of Fluids Engineering., 125, 149-158.

Eynon P. A. and Whitfield A., 2000, Pressure recovery in a turbocharger compressor volute, *Proc. I. Mechanical Engineering Journal of Power and Energy*, 214:6, 599-610.

Gahlot V.K., Seshadri V. and Malhotra, R.C., 1992, Effect of Density, Size Distribution, and Concentration of Solids on the Characteristics of Centrifugal Pumps, *ASME J. Fluids Eng.*, 114. 386-389.

Gandi B.K., Sing S.N. and Seshadri V., 2001, Performance Characteristics of Centrifugal Slurry Pumps. *Journal of Fluids Engineering*, 123, 271-280.

Jafarzadeh B., Hajari A., Alishahi M.M. and Akbari M.H., 2011, The Flow Simulations of a Low Specific-Speed High-Speed Centrifugal Pump, *Applied Mathematical Modelling.*, 35:1, 242-249.

Kadambi J. R., Charoenngam P., Subramanian A., Wernet M.P., Sankovic J. M., Addie G. and Courtwright R., 2004, Investigations of Particle Velocities in a Slurry Pump Using PIV: Part 1, The Tongue and Adjacent Channel Flow, *Journal of Energy Resourches Technology*, 126, 271-278.

Kazim K.A., Maiti B. and Chand P., 1997, Effect of Particle Size, Particle Size Distribution, Specific Gravity and Solids Concentration on Centrifugal Pump Performance, Powder Handl. Process., 9:1, pp. 27-32.

Liu J., Xu Y., Wang D., and Su Q., 2009, Analysis of Liquid-Solid Two Phase Turbulent Flow in FGD System Pump, *CAID & CD, 10th International Conference on IEEE*, November, 615-619.

Mahiwan K., 2000, Study of Flow in Centrifugal Slurry Pump Impeller Using PIV, M.S Thesis, Case Western Reserve University, Cleveland, OH.

Mehta M., 2004, Study of Particulate Flow in the Inra-Blade Channels of a Slurry Pump using Particle Image Velocimetry, M.S Thesis, Case Western Reserve University, Cleveland, OH.

Sellgren A., 1979, Performance of Centrifugal Pumps When Pumping Ores and Industrial Minerals, *Proc. Hydro Transport-6, paper G1, BHRA Fluid Engineering*, 291-304.

Shujia Z., Baolin Z., Qingbo H. and Xianhua L.,2006, Virtual Performance Experiment of a Centrifugal Pump Proceedings of the 16th Int. Conference on Artificial Reality and Telexistence-Workshops (ICAT'06).

Singh J.P., Kumar S. and Mohapatra S. K., 2011, Computational Investigation of Slurry Pump Handling Bottom Ash, *International Journal of Fluids Engineering*, 3:2, 241-249.

Singh J.P., Kumar S. and. Mohapatra S.K., 2011, Computational Investigation of Centrifugal Slurry Pump Handling Bottom Ash, *International Journal of Fluids Engineering*, 3:2, 241-249.

Tufekcioglu Kaucuk Ltd., 2013.

Vocadlo J.J., Koo J.K. and Prang A.J., 1974, Performance of Centrifugal Pumps in Slurry Services, *Proc. Hydro Transport-3, Paper J2, BHRA Fluid Engineering.*

Warman International Ltd., 2000, *Warman Slurry Pumping Handbook*, Australasian Version: Feb., 5-10.

Zhou W., Zhao Z., Lee T.S. and Winoto S.H., 2003, Investigation of Flow Through Centrifugal Pump Impellers Using Computational Fluid Dynamics, *International Journal of Rotating Machinery*, 49-61.

Mehmet Salih CELLEK is an Research Assistant of Mechanical Engineering at Yildiz Technical University, Turkey. He graduated from University of Sakarya in 2010 with a BSME degree. He received a MSc. degree in 2013 in Mechanical Engineering from Sakarya University. He is currently a Ph.D. student in Heat-Prossess Program in Mechanical Engineering at Yildiz Technical University. His main research areas are turbomachinary, combustion, energy audit and recovery system, heat exchangers and CFD. He is married and has one child.

Tahsin ENGİN was born in 1968 in Samsun. He received his BSc. degree in Mechanical Engineering from Hacettepe university in 1992 and MSc. degree in Energy branch from Zonguldak Karaelmas (Bülent Ecevit) University and Ph.D. degree also in Energy branch from Sakarya University. He had been worked in Van Cement between 1992-1994 and he had been in Universiy of Nevada/Reno from 2001 to 2003 for his post doctoral research. At the same time he had been worked as a master in the Energy Assesment Center. He has worked in four projects as an administor and in eight project as an investigators. He has received assosiate Professor degree in 2008 then Professor degree in 2013. He has translated two books (Fluid Dynamics/Differantial Equaiton) and these books are awarded by TUBA for their succesful translation. Tahsin Engin teaches Fluid Mechanics, Differential Equations and Numerical Analysis. He has been working as general menegar in Sakarya Technopolis and manager in ADAPTTO-Tchnology transfer office since 2014. Tahsin Engin has more than 80 printed scientific studies and he is married and has 2 children